Effects of reactant rotation on the dynamics of the OH + CH4 → H2O + CH3 reaction : a six-dimensional study

Song, Hongwei; Li, Jun; Jiang, Bin; Yang, Minghui; Lu, Yunpeng; Guo, Hua

2014

Effects of reactant rotation on the dynamics of the OH + CH4 H2O + CH3 reaction: A six-dimensional study

Hongwei Song, Jun Li, Bin Jiang, Minghui Yang, Yunpeng Lu, and Hua Guo

---

Articles you may be interested in

Six-dimensional and seven-dimensional quantum dynamics study of the OH + CH4 H2O + CH3 reaction
J. Chem. Phys. **139**, 154310 (2013); 10.1063/1.4825100

Kinetic and dynamic studies of the Cl(2 P u) + H2O(X 1 A 1) HCl(X 1+) + OH(X 2) reaction on an ab initio based full-dimensional global potential energy surface of the ground electronic state of ClH2O
J. Chem. Phys. **139**, 074302 (2013); 10.1063/1.4817967

Communication: Full dimensional quantum rate coefficients and kinetic isotope effects from ring polymer molecular dynamics for a seven-atom reaction OH + CH4 CH3 + H2O
J. Chem. Phys. **138**, 221103 (2013); 10.1063/1.4811329

Comprehensive theoretical studies on the CF3H dissociation mechanism and the reactions of CF3H with OH and H free radicals
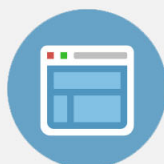J. Chem. Phys. **126**, 034307 (2007); 10.1063/1.2426336

The reactions CH n D 4n + OH P and CH 4 + OD CH 3 + HOD as a test of current direct dynamics computational methods to determine variational transition-state rate constants. I.
J. Chem. Phys. **114**, 2154 (2001); 10.1063/1.1335655

Effects of reactant rotation on the dynamics of the OH + CH$_4$ → H$_2$O + CH$_3$ reaction: A six-dimensional study

Hongwei Song,[1] Jun Li,[1] Bin Jiang,[1] Minghui Yang,[2] Yunpeng Lu,[3,a] and Hua Guo[1,a]

[1]*Department of Chemistry and Chemical Biology, University of New Mexico, Albuquerque, New Mexico 87131, USA*

[2]*Key Laboratory of Magnetic Resonance and Atomic and Molecular Systems, State Key Laboratory of Magnetic Resonance and Atomic and Molecular Physics, Wuhan Centre for Magnetic Resonance, Wuhan Institute of Physics and Mathematics, Chinese Academy of Sciences, Wuhan 430071, People's Republic of China*

[3]*Division of Chemistry and Biological Chemistry, School of Physical and Mathematical Sciences, Nanyang Technological University, Singapore 637371, Singapore*

The dynamics of the hydrogen abstraction reaction between methane and hydroxyl radical is investigated using an initial state selected time-dependent wave packet method within a six-dimensional model. The *ab initio* calibrated global potential energy surface of Espinosa-García and Corchado was used. Integral cross sections from several low-lying rotational states of both reactants have been obtained using the centrifugal sudden and *J*-shifting approximations. On the empirical potential energy surface, the rotational excitation of methane has little effect on the reaction cross section, but excited rotational states of OH inhibit the reactivity slightly. These results are rationalized with the newly proposed sudden vector projection model. © *2014 AIP Publishing LLC*. [http://dx.doi.org/10.1063/1.4866426]

I. INTRODUCTION

Recent advances in both algorithms and computational power have helped quantum dynamical studies to move beyond of the A + BC type reactions.[1–3] Thanks to the larger number of degrees of freedom, dynamics of reactions involving four or more atoms are usually richer and more interesting. However, they are also more challenging for quantum dynamical characterization because of the large size of grid/basis needed to converge the calculations. Except for few cases,[4,5] full-dimensional quantum dynamical studies beyond tetra-atomic reactive systems are almost all based on the multi-configuration time-dependent Hartree approach.[6,7] In the mean time, many quantum scattering work employed reduced-dimensional models, exemplified by studies of the H + CH$_4$,[8–13] O + CH$_4$,[14,15] and OH + CH$_4$ reactions.[16–20] Benchmark studies have so far suggested that properly devised reduced-dimensional models are capable of giving an accurate description of the reaction dynamics.[10]

Polyatomic reactions offer a fertile field for advancing our understanding of a fundamental question in reaction dynamics, namely the relative efficacy of various forms of energy in promoting reactivity. The influence of translational and vibrational modes of reactants have been extensively investigated by many authors,[21–26] and rules of thumb exist.[27–30] However, the effects of reactant rotation are less well understood.[31] This is partly due to the difficulties in experimental preparation of single quantum states as well as the rapidly increasing computational costs for exact quantum calculations. It is interesting to note that there are more than one

rotational degree of freedom for reactive systems with four or more atoms, thus providing a rich testing ground for understanding the rotational effects. Indeed, Zhang and Lee have addressed this question in the H$_2$ + OH[32,33] and H$_2$ + CN reactions.[34] They found that OH rotational excitation mildly enhances the reactivity while H$_2$ rotational excitation inhibits the H$_2$ + OH reaction, and simultaneous rotational excitation of both H$_2$ and OH does not have a correlated effect on dynamics. For the H$_2$ + CN reaction, CN rotational excitations up to seven have essentially no effect on the integral cross section (ICS) while H$_2$ rotational excitation substantially reduces the cross section.

The particular reaction investigated here is that between OH and CH$_4$, which produces H$_2$O and CH$_3$. This is a key reaction in the combustion of hydrocarbon fuels.[35,36] In the troposphere, this reaction represents the major process for the removal of atmospheric methane,[37] which is a greenhouse gas. Experimental rate constants for the reaction have been reported over a wide range of temperatures.[37–40] The rate constant is largely Arrhenius at high temperatures but departs the Arrhenius limit at low temperatures due apparently to tunneling. The state-to-state dynamics of the OH + CD$_4$ reaction has been studied experimentally by Liu and co-workers.[41–43] In addition, the vibrational spectroscopy and decay dynamics of the CH$_4$–OH complex in the entrance channel have been reported by Lester and co-workers.[44,45]

Theoretically, the early attention on the title reaction has been mostly focused on the transition state, rate constants, and kinetic isotope effects.[46–54] There are, however, relatively few dynamics calculations. Nyman and co-workers[16–18] have, for example, investigated the mode selectivity of this reaction under the rotating-line and rotating-bond approximations with

---

a)Authors to whom correspondence should be addressed. Electronic addresses: yplu@ntu.edu.sg and hguo@unm.edu

reduced dimensionality PESs. Subsequently, Yu[19] performed quantum scattering calculations on the global empirical PES of Espinosa-García and Corchado[50] using a five-dimensional model. Very recently, some of the current authors carried out time-dependent wave packet calculations of the OH + CH$_4$ reaction with six and seven-dimensional models,[20] using the same PES of Espinosa-García and Corchado.[50] Here, we extend that work by focusing on the rotational degrees of both reactants. This paper is organized as follows. Section II outlines the theoretical methodology of the initial state selected wave packet method. The results are presented in Sec. III, followed by discussion in Sec. IV. We conclude in Sec. V.

II. THEORY

The initial state selected time-dependent wave packet (ISSWP) method employed in the present study is the same as that in our previous work,[20] which has been well documented.[55] Hence, we only briefly outline aspects related to this reaction.

The CH$_4$ molecule in our reduced-dimensional model is approximated by YCZ$_3$, in which Y is the transferring hydrogen and CZ$_3$ represents the non-reactive methyl group. Both YCZ$_3$ and CZ$_3$ are assumed to maintain the C$_{3v}$ symmetry throughout the reaction.[56] The reactant Jacobi coordinates used in the calculations are shown in Fig. 1. The scattering coordinate R is the distance between the centers of mass (COMs) of OH and YCZ$_3$, r_1 is the distance of OH and is fixed at its equilibrium position ($r_{10} = 1.833\ a_0$), r_2 is the distance between the COM of CZ$_3$ and Y, and r_u is the bond length of CZ in the CZ$_3$ group and is fixed at its equilibrium position ($r_{u0} = 2.067\ a_0$). Neglecting the CZ$_3$ internal rotation, the C$_{3v}$ symmetry axis of CZ$_3$ group, i.e., s, coincides with r_2.

The six-dimensional (6D) Hamiltonian for the OH + YCZ$_3$ system is given by ($\hbar = 1$ hereafter):[20,56]

$$\hat{H} = -\frac{1}{2\mu_R}\frac{\partial^2}{\partial R^2} - \frac{1}{2\mu_{r_2}}\frac{\partial^2}{\partial r_2^2} + \frac{(\hat{J} - \hat{j}_{12})^2}{2\mu_R R^2} + \frac{\hat{j}_1^2}{2\mu_{r_1} r_{10}^2}$$
$$+ \frac{\hat{j}_2^2}{2I_{YCZ_3}} + \hat{K}_{CZ_3}^{vib} + V(R, r_2, \chi, \theta_1, \theta_2, \varphi), \quad (1)$$
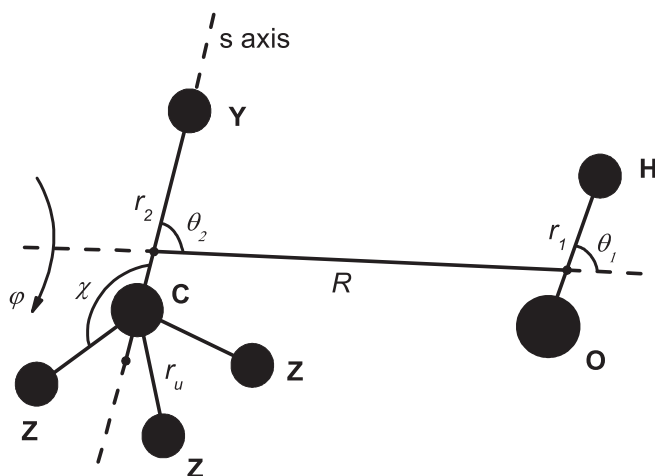

FIG. 1. The seven-dimensional Jacobi coordinates for the OH + YCZ$_3$ system.

where the moment of inertia, $I_{YCZ_3} = \mu_{r_2} r_2^2 + \frac{3}{2}m_Z r_{u0}^2 \sin^2\chi + \frac{3m_C m_Z}{m_C + 3m_Z}r_{u0}^2 \cos^2\chi$, resulting from the consideration that the reactant YCZ$_3$ keeps C$_{3v}$ symmetry. μ_R is the reduced mass between OH and Y-CZ$_3$, μ_{r_1} is the reduced mass of OH, and μ_{r_2} is the reduced mass of Y-CZ$_3$. $\hat{J}$ is the total angular momentum operator of the system and $\hat{j}_{12} = \hat{j}_1 + \hat{j}_2$, where $\hat{j}_1$ is the rotational angular momentum operator of OH, and $\hat{j}_2$ is the rotational angular momentum operator of YCZ$_3$ with respect to the axis perpendicular to the C$_{3v}$ symmetry axis of CZ$_3$ group. In other words, the YCZ$_3$ moiety is approximated as a linear rotor in this model. $\hat{K}_{CZ_3}^{vib}$ is the vibrational kinetic energy operator for the umbrella motion of CZ$_3$ with the bond length of CZ fixed at 2.067 a_0, which is defined as[56]

$$\hat{K}_{CZ_3}^{vib} = -\frac{1}{2r_{u0}^2}\left(\frac{\cos^2\chi}{\mu_x} + \frac{\sin^2\chi}{\mu_s}\right)\frac{\partial^2}{\partial\chi^2}$$
$$-\frac{1}{r_{u0}^2}\left(\frac{1}{\mu_s} - \frac{1}{\mu_x}\right)\sin\chi\cos\chi\frac{\partial}{\partial\chi}, \quad (2)$$

where $\mu_x = 3m_Z$ and $\mu_s = 3m_C m_Z/(m_C + 3m_Z)$.

The parity (ε) adapted time-dependent wave packet is expanded in terms of the body-fixed (BF) rovibrational functions,

$$\psi^{JM\varepsilon}(\vec{R}, \vec{r}_1, \vec{r}_2, \chi, t)$$
$$= \sum_{nv_2 v_\chi j_1 j_2 j_{12}K} F_{nv_2 v_\chi j_1 j_2 j_{12}K}^{JM\varepsilon}(t) u_n(R)\phi_{v_2}(r_2)\phi_{v_\chi}(\chi)$$
$$\times \Phi_{j_1 j_2 j_{12}K}^{JM\varepsilon}(\hat{R}, \hat{r}_1, \hat{r}_2), \quad (3)$$

where n labels the translational basis functions; v_2 and v_χ are the basis indices for r_2 and χ, respectively; j_1 and j_2 are the rotational quantum numbers of OH and YCZ$_3$ moieties. The translational basis function, $u_n^{v_2}$, is dependent on v_2 due to the employment of an L-shaped grid. $\Phi_{j_1 j_2 j_{12}K}^{JM\varepsilon}$ in Eq. (3) is the parity-adapted coupled BF total angular momentum eigenfunction, which can be written as

$$\Phi_{j_1 j_2 j_{12}K}^{JM\varepsilon} = (1 + \delta_{K0})^{-1/2}\sqrt{\frac{2J+1}{8\pi}}$$
$$\times \left[D_{K,M}^{J*}Y_{j_1 j_2}^{j_{12}K} + \varepsilon(-1)^{j_1 + j_2 + j_{12} + J}D_{-K,M}^{J*}Y_{j_1 j_2}^{j_{12}-K}\right], \quad (4)$$

where $D_{K,M}^J$ is the Wigner rotation matrix.[57] M is the projection of total angular momentum J on the space-fixed z axis, and K is the projection on the body-fixed z axis which coincides with R. $Y_{j_1 j_2}^{j_{12}K}$ is the angular momentum eigenfunction of $\hat{j}_{12}$ defined as

$$Y_{j_1 j_2}^{j_{12}K} = \sum_{m_1}\langle j_1 m_1 j_2 K - m_1 | j_{12}K\rangle$$
$$\times y_{j_1 m_1}(\theta_1, 0)y_{j_2 K - m_1}(\theta_2, \varphi) \quad (5)$$

and y_{jm} denotes the spherical harmonics. Note the restriction that $\varepsilon(-1)^{j_1 + j_2 + j_{12} + J} = 1$ for $K = 0$.

Under the centrifugal-sudden (CS) approximation,[58,59] the $(\hat{J} - \hat{j}_{12})^2$ term is given by

$$\left\langle \Phi_{j_1 j_2 j_{12} K}^{JM\varepsilon} \middle| (\hat{J} - \hat{j}_{12})^2 \middle| \Phi_{j_1' j_2' j_{12}' K'}^{JM\varepsilon} \right\rangle$$

$$\approx \delta_{j_1 j_1'} \delta_{j_2 j_2'} \delta_{j_{12} j_{12}'} \delta_{K K'} [J(J+1) + j_{12}(j_{12}+1) - 2K^2]. \tag{6}$$

In other words, K becomes a good quantum number and is conserved. The potential matrix in the angular basis $\Phi_{jK}^{JM\varepsilon}$ can be calculated as

$$\left\langle \Phi_{j_1 j_2 j_{12} K}^{JM\varepsilon} \middle| V \middle| \Phi_{j_1' j_2' j_{12}' K'}^{JM\varepsilon} \right\rangle = 2\pi \delta_{K K'} \left\langle Y_{j_1 j_2}^{j_{12} K} \middle| V \middle| Y_{j_1' j_2'}^{j_{12}' K} \right\rangle. \tag{7}$$

It can be seen that the potential matrix for even parity is identical to that for odd parity for $K > 0$. As both of the potential and centrifugal potential terms are independent of the total parity of the system, $\varepsilon = \pm 1$ yield the same reaction probabilities.[32]

In the calculations, we first construct in the reactant asymptote initial wave packets consisting of a Gaussian wave packet in the scattering coordinate and internal ro-vibrational states of both OH and CH$_4$, denoted by $v_0 = (v_{20}, v_{\chi 0})$ and $j_0 = (j_{10}, j_{20})$. The latter also leads to several possible j_{120} values. These wave packets are propagated in time using the split-operator method.[60] In order to obtain the reaction probability, $P_{v_0 j_0 j_{120} K_0}^{J\varepsilon}(E)$, the flux through the dividing surface, $S[r_2 = r_2^F]$, is obtained from the energy-dependent scattering wavefunction, $\psi_i^+(E)$.

The integral cross section (ICS) from a specific initial state is obtained by summing the reaction probabilities over all the partial waves (total angular momentum J),

$$\sigma_{v_0 j_0}(E) = \frac{1}{(2j_{10}+1)(2j_{20}+1)}$$

$$\times \sum_{j_{120} K_0 \varepsilon} \frac{\pi}{k^2} \sum_{J \geq K_0} (2J+1) P_{v_0 j_0 j_{120} K_0}^{J\varepsilon}(E)$$

$$= \frac{1}{(2j_{10}+1)(2j_{20}+1)} \sum_{j_{120} K_0 \varepsilon} \sigma_{v_0 j_0}^{j_{120} K_0 \varepsilon}(E), \tag{8}$$

where $\sigma_{v_0 j_0}^{j_{120} K_0 \varepsilon}(E)$ is defined as the j_{12}, K and ε specific cross section, and K_0 is taken from 0 to j_{120}. In the case when either j_1 or j_2 equals to zero, j_{12} is the sum of j_1 and j_2 that can only take one value. In this study, we focus on the dynamics from the ground vibrational states, i.e., $v_2 = v_\chi = 0$. Thus, we will drop the indices ε, v_2, v_χ, and j_{12} from now on.

The cross section can also be approximately obtained using the J-shifting (JS) approximation,[61,62] which estimates the reaction probabilities for $J > K$ by simply shifting the collision energy in the probability for $J = K$, i.e., $P^{J > K}(E) = P^{J = K}(E - \Delta E)$, where $\Delta E = B^*[J(J+1) - K(K+1)]$.[63] This approximation is much less costly than the coupled-channel (CC) calculation, but it may introduce significant errors.

III. RESULTS

The numerical parameters employed in the calculations on an L-shaped grid are similar to those used in our previ-

ous work.[20] For the translational coordinate R, 110 sine discrete variable representation (DVR) basis/points are used in the whole range from 3.5 to 12.0 a_0 and 35 sine DVR basis/points are used in the interaction region. For the dissociating C–H bond of r_2, 26 PODVR basis/points are used in the interaction region, and 3 PODVR basis/points are used in the asymptotic region. Twelve PODVR points are used for χ in the range from 0 to π. The angular basis is 42 for $j_{1\text{max}}$ and 43 for $j_{2\text{max}}$, respectively. The center of the initial wave packet is located at 11.0 a_0 and the propagation time is around 18 000 a.u. with a time step of 15 a.u. The flux dividing surface is positioned at $r_2^F = 3.5\ a_0$.

Our calculations are based on the *ab initio* calibrated PES of Espinosa-Carcía and Corchado,[50] which was constructed by augmenting the previous potential function for the H/O + CH$_4$ systems[64,65] with two new terms: a Morse function to describe the O–H bond and a harmonic bending term to describe the H–O–H bending mode. This PES has a linear transition state with a barrier height of 0.34 eV with respect to the reactant asymptote.

A. Comparison of the CS and JS approximations

In our calculations, the reaction probabilities for $J = K$ were obtained under the CS approximation and the probabilities for $J > K$ were obtained using the JS approximation. The rotational constant B^* is taken as 0.28126 cm^{-1}, which is obtained from the geometry of the saddle point of the PES (taken from Table II of Ref. 50). In our previous work, we have tested on the accuracy of the CS and JS approximations by comparing their ICSs with the CC results.[20] It was found that the CS approximation works well over the whole energy range studied, and the JS approximation provides accurate cross sections at low collision energies while overestimates them at relatively high collision energies. However, the test was limited to the case with the ground rovibrational states of the reactants. Here, we extended the comparison to rotationally excited state, i.e., $j_1 = 0$, $j_2 = 4$, and $K = 2$. The calculations were, however, performed only under the CS and/or JS approximations, because a CC calculation is prohibitively expensive.

Figure 2 shows the CS and JS probabilities for the OH ($j_1 = 0$) + CH$_4$ ($j_2 = 4$) reaction with $J = 30$, 60, 90, and 120 and $K = 2$ as a function of translational energy. The CS probability for $J = 2$ and $K = 2$ is given for comparison. As can be seen from the figure, the JS probability for $J = 30$ is quite similar to the CS probability over the whole energy range. As J increases, however, the difference between the CS and JS probabilities increases. It appears that the JS approximation gives a good estimation of the energy threshold while it overestimates the reaction probability in higher energy range.

In Fig. 3, we present the CS and JS ICSs for the OH($j_1 = 0$) + CH$_4$($j_2 = 4$) reaction. It is apparent that the JS cross sections resemble the CS ones near the reaction threshold. As the collision energy increases, the JS approximation increasingly overestimates the ICS, with the relative error up to 30%. These conclusions are generally consistent with the findings from the ground rovibrational states of the reactants.
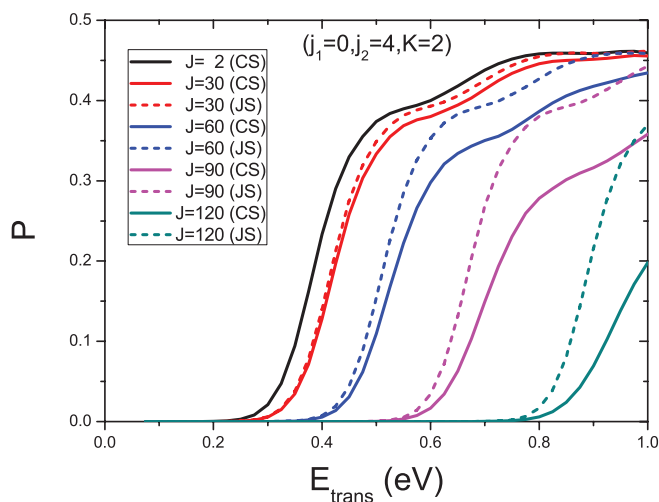
FIG. 2. The comparison of the CS and *JS* probabilities for the OH($j_1 = 0$) + CH$_4$($j_2 = 4$) reaction with $J = 2$, 30, 60, 90, and 120 and $K = 2$ as a function of translational energy.

Considering that the *JS* approximation is based on a very simple physical model, its performance is quite acceptable for this reaction. As the *JS* approximation greatly reduces the computational costs, the results below were all calculated with this approximation.

B. OH rotational excitation

Figure 4 shows the *K*-specific and averaged *JS* ICSs for the OH($j_1 = 1, 3, 5$) + CH$_4$($j_2 = 0$) reaction as a function of collision energy. For $K = 0$, the initial state exists only in even total parity, while for $K > 0$, it exists in both even and odd total parities. However, the two total parities give the same cross section under the CS approximation. The *K* dependence of the ICSs $\sigma_{j_1=1}^K$ is shown in the upper panel of Fig. 4. Clearly, $\sigma_{j_1=1}^{K=1}$ is substantially larger than $\sigma_{j_1=1}^{K=0}$ in the energy range above the threshold. For $j_1 = 3$ and 5, as shown
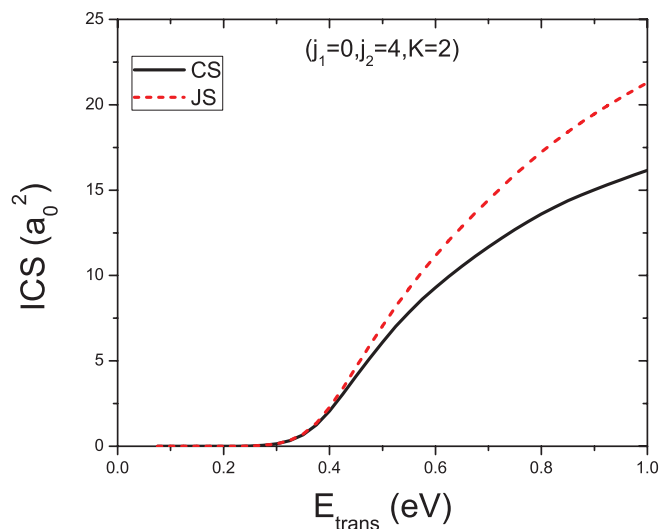

FIG. 4. The *K*-specific and averaged *JS* ICSs for the OH($j_1 = 1, 3, 5$) + CH$_4$($j_2 = 0$) reaction as a function of translational energy.

in the central and lower panels of the same figure, respectively, the cross section increases with the value of *K*, i.e., $\sigma_{j_1=3}^{K=3} > \sigma_{j_1=3}^{K=2} > \sigma_{j_1=3}^{K=1} > \sigma_{j_1=3}^{K=0}$ and $\sigma_{j_1=5}^{K=5} > \sigma_{j_1=5}^{K=4} > \sigma_{j_1=5}^{K=3} > \sigma_{j_1=5}^{K=2} > \sigma_{j_1=5}^{K=1} > \sigma_{j_1=5}^{K=0}$. This trend also holds for $j_1 = 2$ and 4.

The *JS* ICSs for the OH($j_1 = 0$–5) + CH$_4$($j_2 = 0$) reaction are plotted in Figs. 5(a) and 5(b) as a function of translational and total energy, respectively. From Fig. 5(a), we can see that the rotational excitation of OH clearly inhibits the reaction, at least when $j_1 \leq 5$. Although the OH rotation has almost no effect on the energy threshold and the cross section profiles are similar to each other from different rotational states, the amplitudes are quite different. The ICS decreases with the increase of the value of j_1, in sharp contrast to the effect of OH rotation in the OH + H$_2$ reaction[32] where OH rotation excitation mildly enhances the cross section. The different behavior can be traced to the *K* dependence. It was found that in the diatom-diatom reactions the cross section first increases and then decreases with the increase of *K* for $K > 2$. In the OH + CH$_4$ reaction, the cross section, however, has a monotonically increasing *K* dependence. In Fig. 5(b), the ICSs are plotted as a function of total energy. Obviously, the rotational energy of OH is less efficient than translational energy in promoting the reaction. This conclusion is consistent with the 3D results of Nyman and Clary on a model PES[16] and 5D results of Yu using the same PES.[19] It appears that these reduced dimensional models have captured the essence of the dynamics.

FIG. 3. Comparison of the CS and *JS* ICSs for the OH($j_1 = 0$) + CH$_4$($j_2 = 4$) reaction with $K = 2$ as a function of translational energy.
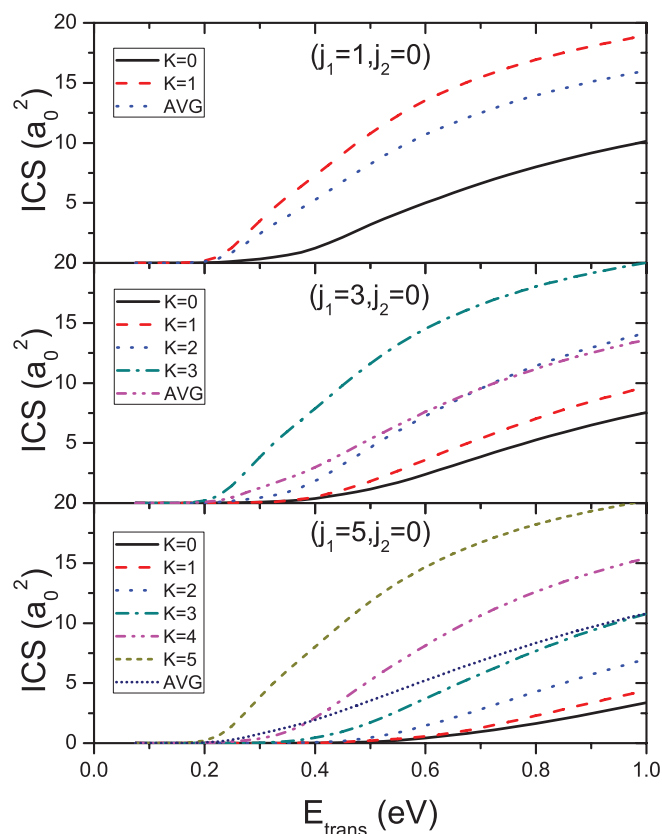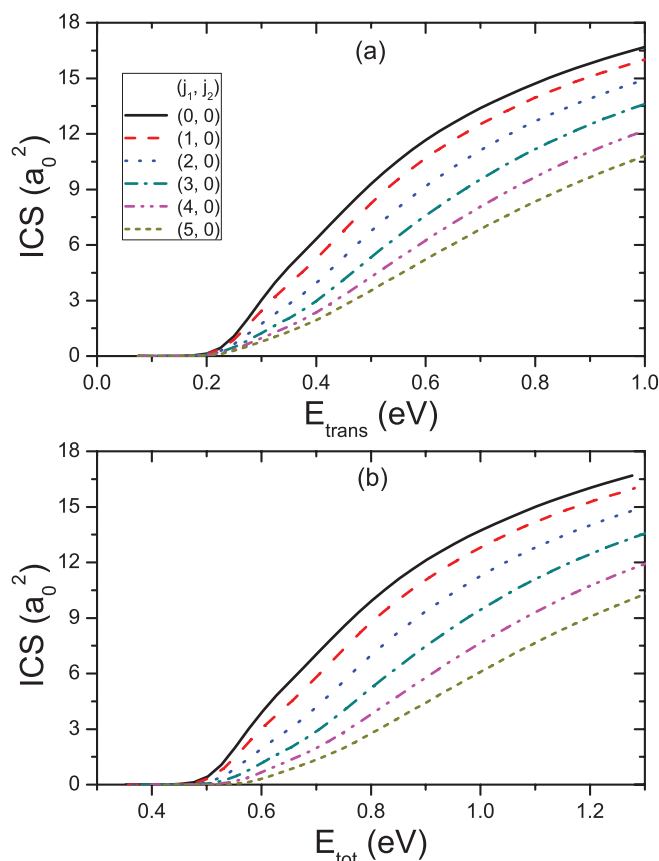
FIG. 5. The averaged JS ICSs for the OH($j_1 = 0$–5) + CH$_4$($j_2 = 0$) reaction as a function of (a) translational energy and (b) total energy.

FIG. 6. The K-specific and averaged JS ICSs for the OH($j_1 = 0$) + CH$_4$($j_2 = 1, 3, 5$) reaction as a function of translational energy.

C. CH$_4$ rotational excitation

In Fig. 6, we present the K-specific and averaged JS ICSs for the OH($j_1 = 0$) + CH$_4$($j_2 = 1, 3, 5$) reaction. It can be seen that the cross section decreases with the increase of K over the entire energy range except that $\sigma_{j_2=3}^{K=1} > \sigma_{j_2=3}^{K=0}$ at high collision energies above about 0.8 eV. We also examine the K dependence of the ICSs for $j_2 = 2$ and 4. They show the same behavior as those for $j_2 = 1, 3$, and 5. The K dependence for CH$_4$ rotational excitation is clearly different from that for OH rotational excitation. Interestingly, it is similar to the K dependence of H$_2$ rotational excitation in the OH + H$_2$ reaction.[32]

The averaged JS ICSs for the OH($j_1 = 0$) + CH$_4$($j_2 = 0$–5) reaction are plotted in Figs. 7(a) and 7(b) as a function of translational and total energy, respectively. It can be seen from Fig. 7(a) that the rotational excitation of CH$_4$ has a very mild inhibition effect. The ICSs for $j_2 = 0, 1$, and 2 are almost indistinguishable. For the six different initial states studied here, they give nearly the same energy threshold. This is different from that of H$_2$ rotational excitation in the OH + H$_2$ reaction,[32,33] in which the rotational excitation of H$_2$ presents a large inhibition effect. The ICSs are plotted as a function of total energy in Fig. 7(b). Obviously, the rotational energy of CH$_4$ is slightly less efficient than translational energy. However, we note that the approximate treatment of the CH$_4$ rotation as a linear rotor serves as a caveat on the aforementioned conclusion as this approximation assumes its ro-
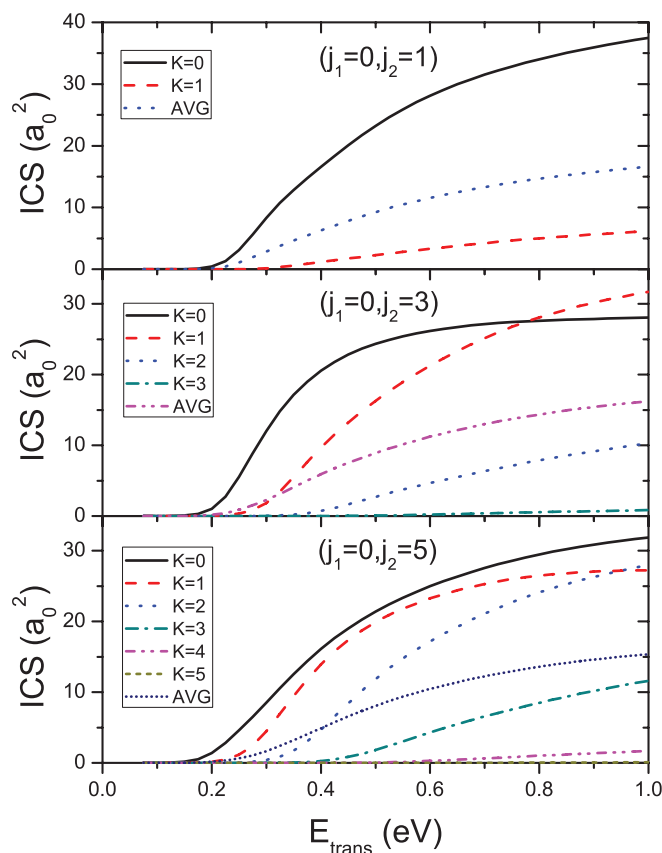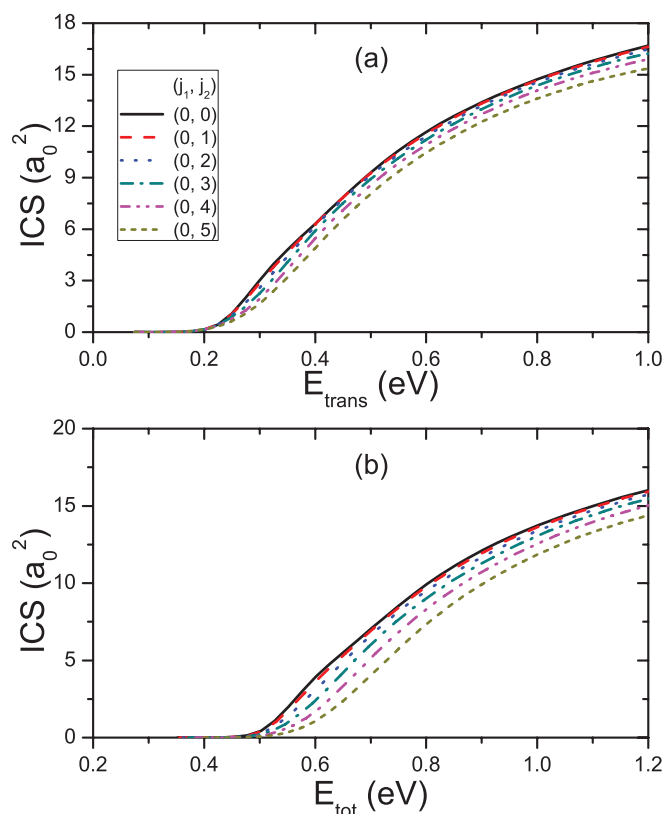

FIG. 7. The averaged JS ICSs for the OH($j_1 = 0$) + CH$_4$($j_2 = 0$–5) reaction as a function of (a) translational energy and (b) total energy.

tational angular momentum vector is always perpendicular to the breaking C–H bond and no rotation along the C–H bond.

IV. DISCUSSION

To understand the dependence of the reactant rotational excitations in this reaction, we resort to the recently proposed Sudden Vector Projection (SVP) model.[29–31] Based on the premise that the rate for intramolecular vibrational energy redistribution (IVR) is longer than the collision time, SVP attributes the efficacy of a reactant mode in promoting the reaction to its coupling with the reaction coordinate at the transition state. Such a coupling is quantified by the overlap between the reactant normal mode ($\vec{Q}_i$) and the reaction coordinate vector ($\vec{Q}_{RC}$): $P_i = \vec{Q}_i \cdot \vec{Q}_{RC} \in [0, 1]$. It has been shown that the SVP model correctly predicted the trends in reactions involving diatomic, triatomic, and penta-atomic reactants.[29–31,66,67] The details for the determination of the vectors ($\vec{Q}$), including those for the reactant rotation, have been given in our earlier work.[29–31]

The SVP values for the reactant modes on the empirical PES of Espinosa-García and Corchado are listed in Table I. It is clear that the symmetric stretching mode of CH_4 has the largest efficacy in promoting the reaction. This is followed by the antisymmetric stretching mode. The reaction is also readily enhanced by the translational mode. The two bending modes of CH_4 and the OH stretching mode have negligible overlaps with the reaction coordinate, thus having limited capacity to enhance the reaction. These conclusions are consistent with the results presented in our earlier paper on this reaction,[20] as well as earlier work.[16,19,50] Interestingly, the SVP values for the rotational degrees of freedom of both reactants also suggest near orthogonality with the reaction coordinate. This is consistent with the results presented above. The inhibitory effects of the reactant rotational excitation can be attributed to the so-called "dis-orienting" effect, which attributes the lower reactivity of rotationally excited reactants to their difficulties to enter the cone of acceptance.[68–70]

However, the conclusions reached by the quantum dynamical studies reported here may not be definitive, as the PES used in the calculations is empirical in nature. To illustrate the possible deficiencies of the PES, we compare in

TABLE I. SVP projections ($P_i = \vec{Q}_i \cdot \vec{Q}_{RC}$) on the PES of Espinosa-García and Corchado and based on *ab initio* calculations (UCCSD(T)-F12a/AVTZ).

Species	PES	*Ab initio*	Mode[a]
CH_4	0.289	0.344	Asymmetric stretch
	0.471	0.425	Symmetric stretch
	0.015	0.013	Rock bend
	0.011	0.087	Umbrella bend
	0.001	0.096	In-plane rotation
	0.000	0.000	Out-of-plane rotation
OH	0.002	0.016	Stretch
	0.034	0.128	Rotation
CH_4–OH	0.265	0.431	Translation
	0.000	0.000	Relative rotation

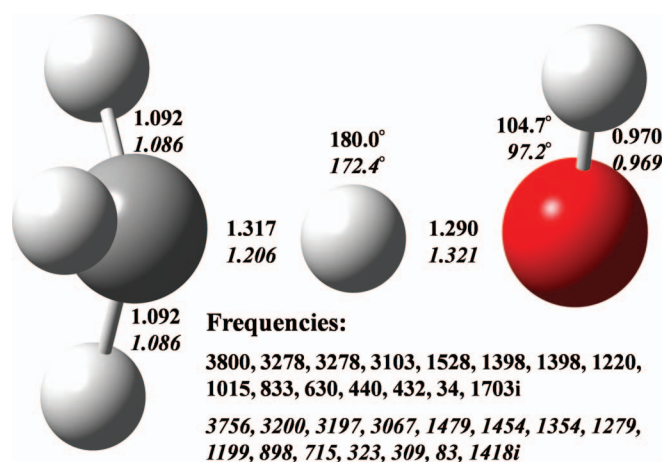[a]For degenerate modes, the average is used.

FIG. 8. The saddle point geometry for the title reaction determined at the CCSD(T)-F12a/AVTZ level of theory. The corresponding PES and *ab initio* values for the bond lengths (Å), bond angles (degree), and harmonic frequencies (cm^{-1}) are listed in normal and italic fonts, respectively.

Fig. 8 the transition-state geometry obtained using an explicitly correlated version of the unrestricted couple cluster singles, doubles and perturbative triples method with the correlation corrected augmented valence triple zeta basis set (UCCSD(T)-F12a/AVTZ)[71,72] with that calculated from the PES. This level of theory has been shown to provide complete basis set quality.[73] Significant differences are found in the saddle point geometries: The *ab initio* OHC angle is less than 180° while that on the PES is collinear, the *ab initio* HOH angle is smaller than that on the PES, and the distances between the transferring H and the two heavy atoms are significantly different from those on the PES. In addition, the imaginary frequency at the saddle point is overestimated by the PES. These differences raise a serious question concerning the accuracy of the PES and suggest the need to construct a more accurate global PES based on a large number of high-level *ab initio* points.

To predict the mode selectivity with the *ab initio* saddle point, we have computed the corresponding SVP values, which are also listed in Table I. The overall agreement between the PES and *ab initio* values is good, but there are some quantitative differences. In particular, we note that the rotational modes of the two reactants appear to be more strongly coupled with the reaction coordinate. As a result, the conclusions based on the empirical PES might need some modifications.

V. CONCLUSIONS

In this work, we have studied the effect of reactant rotation on the dynamics of the OH + CH_4 reaction using the initial state selected time-dependent wave packet method. The calculation has been carried out on an empirical global PES within a reduced six-dimensional model. The accuracy of the *J*S approximation for rotationally excited states of the reactants was assessed by comparing its ICSs with the CS results. It was found that the *J*S model performs well at low collision energies just above the energy threshold while it obviously overestimates the CS ICSs at high collision energies.

Within the JS model, it is found that the rotational energy of OH is less efficient than translational energy in promoting the reaction. For the initial states $j_1 = 1, 2, 3, 4$, and 5, they all present a monotonic increasing K dependence over the whole energy range studied. On the other hand, the rotational excitation of CH_4 is slightly less efficient than translational energy. Interestingly, they present a completely different K dependence with respect to the rotational excitation of OH. For $j_2 = 1, 2, 3, 4$, and 5, they give a monotonic decreasing K dependence at low and moderate collision energies. The low efficacies of the rotational degrees of freedom of the two reactants are attributed based on the SVP model to their lacks of coupling with the reaction coordinate of this reaction.

However, it needs to be pointed out that the PES used in this work is not sufficiently accurate to yield definitive conclusions concerning the mode selectivity in this reaction. High-level *ab initio* determination of the reaction saddle point uncovered substantial inaccuracies in the PES, which underscores the urgent need to develop quantitatively accurate global PES for this prototypical reaction.

ACKNOWLEDGMENTS

[1] S. C. Althorpe and D. C. Clary, Annu. Rev. Phys. Chem. **54**, 493 (2003).

[2] H. Guo, Int. Rev. Phys. Chem. **31**, 1 (2012).

[3] G. Nyman and H.-G. Yu, Int. Rev. Phys. Chem. **32**, 39 (2013).

[4] D. Wang, J. Chem. Phys. **124**, 201105 (2006).

[5] M. Yang, J. Chem. Phys. **129**, 064315 (2008).

[6] U. Manthe, Mol. Phys. **109**, 1415 (2011).

[7] H.-D. Meyer, F. Gatti, and G. A. Worth, *Multidimensional Quantum Dynamics: MCTDH Theory and Applications* (Wiley-VCH, 2009).

[8] M. Yang, D. H. Zhang, and S.-Y. Lee, J. Chem. Phys. **117**, 9539 (2002).

[9] L. Zhang, Y. Lu, S.-Y. Lee, and D. H. Zhang, J. Chem. Phys. **127**, 234313 (2007).

[10] G. Schiffel and U. Manthe, J. Chem. Phys. **132**, 084103 (2010).

[11] W. Zhang, Y. Zhou, G. Wu, Y. Lu, H. Pan, B. Fu, Q. Shuai, L. Liu, S. Liu, L. Zhang, B. Jiang, D. Dai, S.-Y. Lee, Z. Xie, B. J. Braams, J. M. Bowman, M. A. Collins, D. H. Zhang, and X. Yang, Proc. Natl. Acad. Sci. U.S.A. **107**, 12782 (2010).

[12] Y. Zhou, C. Wang, and D. H. Zhang, J. Chem. Phys. **135**, 024313 (2011).

[13] S. Liu, J. Chen, Z. Zhang, and D. H. Zhang, J. Chem. Phys. **138**, 011101 (2013).

[14] M. Yang, S.-Y. Lee, and D. H. Zhang, J. Chem. Phys. **126**, 064303 (2007).

[15] R. Liu, M. Yang, G. Czakó, C. T. Bowman, J. Li, and H. Guo, J. Phys. Chem. Lett. **3**, 3776 (2012).

[16] G. Nyman and D. C. Clary, J. Chem. Phys. **101**, 5756 (1994).

[17] G. Nyman, D. C. Clary, and R. D. Levine, Chem. Phys. **191**, 223 (1995).

[18] G. Nyman, Chem. Phys. Lett. **240**, 571 (1995).

[19] H. G. Yu, J. Chem. Phys. **114**, 2967 (2001).

[20] H. Song, S.-Y. Lee, M. Yang, and Y. Lu, J. Chem. Phys. **139**, 154310 (2013).

[21] R. N. Zare, Science **279**, 1875 (1998).

[22] F. F. Crim, Acc. Chem. Res. **32**, 877 (1999).

[23] S. Yan, Y. T. Wu, B. Zhang, X.-F. Yue, and K. Liu, Science **316**, 1723 (2007).

[24] W. Zhang, H. Kawamata, and K. Liu, Science **325**, 303 (2009).

[25] G. Czakó and J. M. Bowman, Science **334**, 343 (2011).

[26] Z. Zhang, Y. Zhou, D. H. Zhang, G. Czakó, and J. M. Bowman, J. Phys. Chem. Lett. **3**, 3416 (2012).

[27] J. C. Polanyi, Science **236**, 680 (1987).

[28] S. Yan, Y.-T. Wu, and K. Liu, Proc. Natl. Acad. Sci. U.S.A. **105**, 12667 (2008).

[29] B. Jiang and H. Guo, J. Chem. Phys. **138**, 234104 (2013).

[30] B. Jiang and H. Guo, J. Am. Chem. Soc. **135**, 15251 (2013).

[31] B. Jiang, J. Li, and H. Guo, J. Chem. Phys. **140**, 034112 (2014).

[32] D. H. Zhang and S.-Y. Lee, J. Chem. Phys. **109**, 2708 (1998).

[33] D. H. Zhang and S. Y. Lee, J. Chem. Phys. **110**, 4435 (1999).

[34] D. H. Zhang and S.-Y. Lee, J. Chem. Phys. **112**, 203 (2000).

[35] I. Glassman, *Combustion*, 3rd ed. (Academic Press, San Diego, Califonia, 1996).

[36] I. M. Campbell, *Energy and the Atmosphere* (John Wiley & Sons Ltd., London, UK, 1977).

[37] G. L. Vaghjiani and A. R. Ravishankara, Nature (London) **350**, 406 (1991).

[38] K. Yamasaki, A. Watanabe, T. Kakuda, N. Ichikawa, and I. Tokue, J. Phys. Chem. A **103**, 451 (1999).

[39] N. K. Srinivasan, M. C. Su, J. W. Sutherland, and J. V. Michael, J. Phys. Chem. A **109**, 1857 (2005).

[40] D. L. Baulch, C. J. Cobos, R. A. Cox, C. Esser, P. Frank, T. Just, J. A. Kerr, M. J. Pilling, J. Troe, R. W. Walker, and J. Warnatz, J. Phys. Chem. Ref. Data **21**, 411 (1992).

[41] B. Zhang, W. C. Shiu, J. J. Lin, and K. P. Liu, J. Chem. Phys. **122**, 131102 (2005).

[42] B. Zhang, W. C. Shiu, and K. Liu, J. Phys. Chem. A **109**, 8983 (2005).

[43] B. Zhang, W. C. Shiu, and K. Liu, J. Phys. Chem. A **109**, 8989 (2005).

[44] M. D. Wheeler, M. Tsiouris, M. I. Lester, and G. Lendvay, J. Chem. Phys. **112**, 6590 (2000).

[45] M. Tsiouris, M. D. Wheeler, and M. I. Lester, J. Chem. Phys. **114**, 187 (2001).

[46] T. N. Truong and D. G. Truhlar, J. Chem. Phys. **93**, 1761 (1990).

[47] K. D. Dobbs, D. A. Dixon, and A. Komornicki, J. Chem. Phys. **98**, 8852 (1993).

[48] V. S. Melissas and D. G. Truhlar, J. Chem. Phys. **99**, 1013 (1993).

[49] J. C. Corchado, E. L. Coitino, Y. Y. Chuang, P. L. Fast, and D. G. Truhlar, J. Phys. Chem. A **102**, 2424 (1998).

[50] J. Espinosa-García and J. C. Corchado, J. Chem. Phys. **112**, 5731 (2000).

[51] L. Masgrau, A. Gonzalez-Lafont, and J. M. Lluch, Theor. Chem. Acc. **108**, 38 (2002).

[52] B. A. Ellingson, J. Pu, H. Lin, Y. Zhao, and D. G. Truhlar, J. Phys. Chem. A **111**, 11706 (2007).

[53] W. Wang and Y. Zhao, J. Chem. Phys. **137**, 214306 (2012).

[54] J. W. Allen, W. H. Green, Y. Li, H. Guo, and Y. V. Suleimanov, J. Chem. Phys. **138**, 221103 (2013).

[55] J. Z. H. Zhang, *Theory and Application of Quantum Molecular Dynamics* (World Scientific, Singapore, 1999).

[56] J. Palma and D. C. Clary, J. Chem. Phys. **112**, 1859 (2000).

[57] R. N. Zare, *Angular Momentum* (Wiley, New York, 1988).

[58] R. T. Pack, J. Chem. Phys. **60**, 633 (1974).

[59] P. McGuire and D. J. Kouri, J. Chem. Phys. **60**, 2488 (1974).

[60] J. A. Flect, Jr., J. R. Morris, and M. D. Feit, Appl. Phys. **10**, 129 (1976).

[61] J. M. Bowman, J. Phys. Chem. **95**, 4960 (1991).

[62] D. H. Zhang and J. Z. H. Zhang, J. Chem. Phys. **110**, 7622 (1999).

[63] D. H. Zhang, J. C. Light, and S.-Y. Lee, J. Chem. Phys. **109**, 79 (1998).

[64] M. J. D. Jordan, K. C. Thompson, and M. A. Collins, J. Chem. Phys. **102**, 5647 (1995).

[65] J. C. Corchado, J. Espinosa-García, O. Roberto-Neto, Y.-Y. Chuang, and D. G. Truhlar, J. Phys. Chem. A **102**, 4899 (1998).

[66] B. Jiang, R. Liu, J. Li, D. Xie, M. Yang, and H. Guo, Chem. Sci. **4**, 3249 (2013).

[67] B. Jiang and H. Guo, J. Phys. Chem. C **117**, 16127−16135 (2013).

[68] M. Karplus, R. N. Porter, and R. D. Sharma, J. Chem. Phys. **43**, 3259 (1965).

[69] R. D. Levine, J. Phys. Chem. **94**, 8872 (1990).

[70] F. J. Aoiz, L. Bañares, and V. J. Herrero, Int. Rev. Phys. Chem. **24**, 119 (2005).

[71] T. B. Adler, G. Knizia, and H.-J. Werner, J. Chem. Phys. **127**, 221106 (2007).

[72] G. Knizia, T. B. Adler, and H.-J. Werner, J. Chem. Phys. **130**, 054104 (2009).

[73] D. Feller and K. A. Peterson, J. Chem. Phys. **139**, 084110 (2013).